SVPWM Control based Bridgeless PFC Cuk Converter for PMSM under Dynamic Conditions

R. SANKARGANESH[1], S. THANGAVEL[2]

[1]Assistant Professor / EEE, K.S.R. College of Engineering, [2]Professor / EEE, K.S.Rangasamy College of Technology
[1] Tiruchengode, Tamilnadu
INDIA
[1]sankarped@gmail.com
[2]golds71@yahoo.com

Abstract: - The widely used converter models in most of the power electronics and power system applications are the DC-DC converter models. Increase in switching losses has been observed in Conventional Diode Bridge Rectifier (DBR) and hence the researchers are more focused towards bridgeless converters. The design of a novel bridgeless cuk converter model with buck mode operation is focused in this work. In this converter model, four different modes of operations with two modes in positive cycle (switch ON and OFF condition) and two modes in negative cycles with (switch ON and OFF condition) were analyzed. The design of cuk converter with outer voltage control and inner current control integrated with the Power Factor Correction (PFC) analysis is also dealt in this study. Integration of Permanent Magnet Synchronous Motor (PMSM) load and Sensorless Space Vector Pulse Width Modulation (SVPWM) vector with this design is also proposed to control the PMSM. The performance is analyzed for load varying and speed varying conditions using MATLAB and the results are simulated. The results showed that the proposed system provides significant results with cost effective components utilities.

Key-Words: - Cuk Converter, Power Factor Correction, Permanent Magnet Synchronous Motor, Space Vector Pulse Width Modulation, Total Harmonic Distortion (THD)

1 Introduction

The efficiency of renewable energy resources and DC-DC converters has made it suitable for several engineering applications. Various researches on the extraction of the maximum power from the PV panel through suitable converters have been done so far. It is well-known that renewable energy sources may not be suitable in high voltage applications due to high capital cost of the PV panel. Hence, available AC power supplies (i.e., single phase 230 V; three phase 440 V) is utilized in high voltage applications.

Mostly the unregulated dc voltage which are been rectified are employed as an input for these converters however it suffers from the fluctuation because of the line voltage magnitude [1]. Using voltage- and current-control techniques, industries are adopting the various proposed control methods for AC-DC converters

Among many control methods, power supplies with active Power Factor Correction (PFC) techniques are gaining more potential for several types of electronic equipment to work in harmony with the regulations. Even though a boost converter is often used at the front end of most the PFC rectifiers, only lower efficiency having significant losses in the diode bridge [2] is evident in conventional PFC schemes.

The generation losses of the number of semiconductors could be reduced basically by eliminating the full bridge input diode rectifier and therefore numerous research works are being focused on design of bridgeless PFC circuits for maximizing the power supply efficiency. In this type of rectifier, the current is allowed to flow through a lesser number of switching devices rather than the conventional PFC rectifier. This helps in significantly reducing the conduction losses of the converter thus achieving higher efficiency in minimum cost. In order to improve the rectifier power density and/or reduce noise emissions by means of soft-switching techniques or coupled magnetic topologies [3], [4] several bridgeless PFC rectifiers are introduced. Further, some of the limitations of the conventional boost converter like high output DC voltage than peak input voltage, lack of galvanic isolation, and high start-up inrush currents are also evident in the bridgeless boost rectifier [5], [6]. Therefore, to step-down the voltage, an additional converter or an isolation transformer is required [7] for low-output voltage

applications in telecommunication or computer industry.

Recently, such types of converters are receiving a great attention as they are applied in various fields like power supplies for personal computers, office equipments, appliance control, telecommunication equipments, DC motor drives, automotive, aircraft and so on. The key factors considered for the converters selection are the analysis, control and stabilization of switching converters. There are many control methods for controlling the switch mode of AC-DC converters however; in particular the controller of lower cost is much in demand for most of the industrial and high performance applications.

Based on the merits and demerits of each control methods, a particular appropriate control method is been chosen among various methods under specific conditions [8]. The speed control of a DC series motor supplied by Photovoltaic (PV) system is presented in [9]. This design problem of speed controller is modelled as an optimization problem. Bacteria Foraging Optimization Algorithm (BFOA) is deployed to look for optimal Proportional Integral (PI) parameters such as k_p & k_i values of speed controller by minimizing the time domain objective function. The performance of this approach has been validated based on the load torque variation, ambient temperature and radiation. Simulation results have shown significance of this approach in controlling the speed of DC series motor under various disturbances.

A design of a PI controller using Particle Swarm Optimization (PSO) to control the speed of an Induction Motor supplied from wind turbine is presented in [10]. The wind turbine operates as a chief mover to a coupled DC generator. PWM is used to attain the three phase AC voltage from the output of DC generator. This control design is formulated as an optimization problem. PSO has been used to find the optimal controller parameters by minimizing the time domain objective function. The performance of the technique has been validated with respect to the variation of load torque and speed wind turbine. Moreover, the performance of the PSO tuned controller is compared with Genetic Algorithm (GA) tuned controller in order to illustrate the efficiency of the proposed PSO in tuning PI controller.

The speed control of a permanent magnet DC motor drive through Pulse Width Modulation (PWM) and a DC/DC converter is presented in [11]. Particle Swarm Optimization (PSO) technique is used to minimize a time domain objective function and obtain the optimal controller parameters. Load

torque variations have been focused for investigating the performance of the overall system. Simulation results showed the robustness of the controller and performance of the technique for controlling the speed of permanent magnet motors.

Always the control method best performed under any conditions is considered as the best and demanding. A perfect converter model is thus highly required for obtaining high performance control of AC-DC converter. The load factor which is the most variable part of the control system plays a key role affecting the dynamics and hence load is regarded as one of the considerable part of the converter.

A topology proposed consists of common input stage and parallel output stages [12]. It utilizes one control signal over the whole line cycle. In addition, the proposed converter exhibits low inrush current and low magnetic emissions as classical Cuk topology. In [13] proposed topologies are designed to work in discontinuous conduction mode (DCM) to achieve al-most a unity power factor and least value of harmonic distortion in the input current. In various applications of PFC, importance of Cuk converter is understood by its natural protection against inrush current occurring at start-up or overload current, lower input current ripple and the reduced electromagnetic interference (EMI) associated with the discontinuous conduction mode (DCM) topology [14], [15].

In [16] proposed method based on the bridgeless single-phase Ac–Dc Power Factor Correction (PFC) converters with Fuzzy Logic Controller. The proposed topologies are designed to work in Discontinuous Conduction Mode (DCM) to achieve a unity power factor and low total harmonic distortion of the input current. Additional reduction in the size of the PFC inductor and EMI filter is necessary. In [14] presented the digital simulation of single phase AC-DC Bridgeless Cuk for Power Factor Correction (PFC) rectifiers. A conventional Cuk PFC rectifier suffers from high conduction losses due to presence of input rectifier bridges. Due to the lower conduction and switching losses, the proposed topologies can further improve the conversion efficiency.

Among the basic converter topologies, the Cuk converter seems to be highly potential for applications requiring a low current ripple at the input and output ports of the converter, thus, this paper clearly investigates the functionality of the bridgeless cuk converter operated in buck mode with constant DC voltage. Moreover, in order to deal with the PFC, outer voltage control and inner current control operations have been deployed. The proposed converter works in the DCM operation

which gives zero current turn ON in the power switches and zero current turn OFF in the output diode.

2 Proposed System

The overall proposed architectural framework is shown in Fig. 1. The performance of the bridgeless cuk converter is analyzed with the PMSM in the load side.

Power Factor Correction is carried out in the input side based on the power factor control technique (outer voltage control and the inner current control). The load side control of the system is made through sensorless speed estimation and current vector control with Space Vector Pulse Width Modulation (SVPWM) technique.

2.1 Principle of Operation of Proposed Bridgeless Cuk Converter Model

Fig. 2 and Fig. 3 show the conventional bridgeless Cuk converter and proposed bridgeless cuk converter model respectively. The proposed bridgeless cuk converter model shown in Fig. 3 utilizes lesser components when compared with the conventional cuk converter circuit. Moreover, in the proposed converter model, in order to maintain a constant 48 Volt, for a 110 $V_{(rms})$, a closed loop power factor Control has been adopted.

Table 1 shows the device utility comparison of the conventional and the proposed model. The power devices, active and passive components such as switches, diodes, capacitors, inductors and snubber diode are taken for consideration. It is clearly observed that, the proposed converter model utilizes very lesser devices when compared with the conventional cuk converter model. Thus, the proposed converter model is cost effective with reduced switching losses when compared with conventional model.
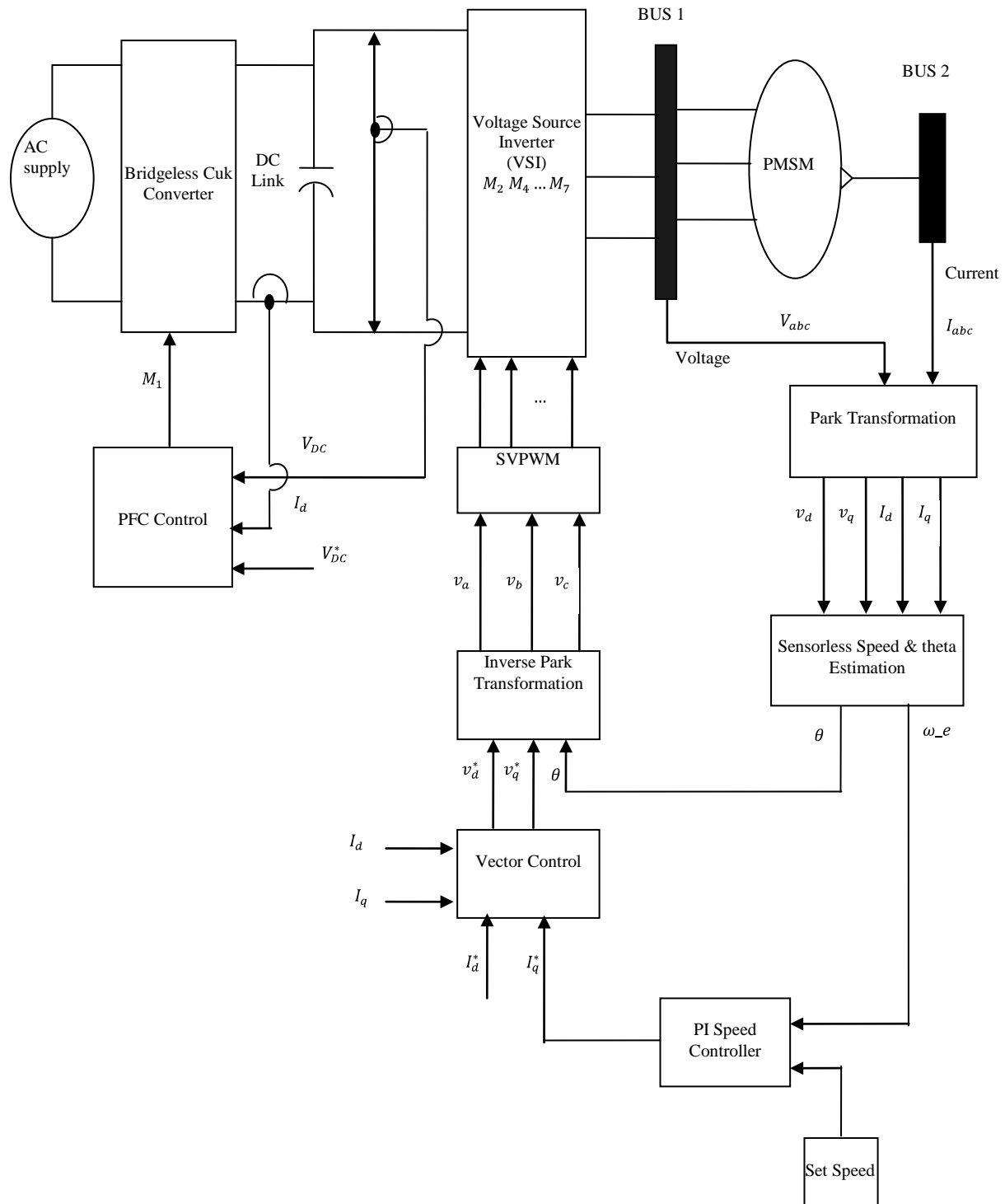
Fig.1. Proposed System Model

Design Model of Inductors and Capacitors

$$L = \frac{V_{dcmin}^2}{P_{min}} * \frac{(1 - d_{min})^2}{2 * f_s}$$

$$L = 92.16 \mu H$$

Here, only 1/10th of the minimum inductance value 'L' will be considered for the proposed converter model. Where $V_{dcmin} = 24\,V$ is denotes the low voltage operating condition of the PMSM considered. $P_{min} = 40\,W$ is the minimum power of PMSM considered at constant 4 Nm torque

condition. $d_{min} = 0.2$ is the worst case duty ratio considered for this approach. $f_s = 50\,KHz$ which is the switching frequency which minimizes the current ripples considerably [19].

$$C_0 = \frac{\frac{P_0}{V_{DC}^*}}{2\omega\,\Delta V_{DC}}$$

$$C_0 = C_{01} + C_{02} = 4644.37\,\mu F$$

Hence, the nearest possible value of 5000 µF is chosen for this approach.

$P_0 = 280\,W$ is the output power considered in this work, $V_{DC}^* = 48\,V$ is the set voltage, $\omega = 2\pi f =$

314 is the angular frequency and $\Delta V_{DC} = 2\%$ is the ripple dc link voltage considered for this proposed approach.
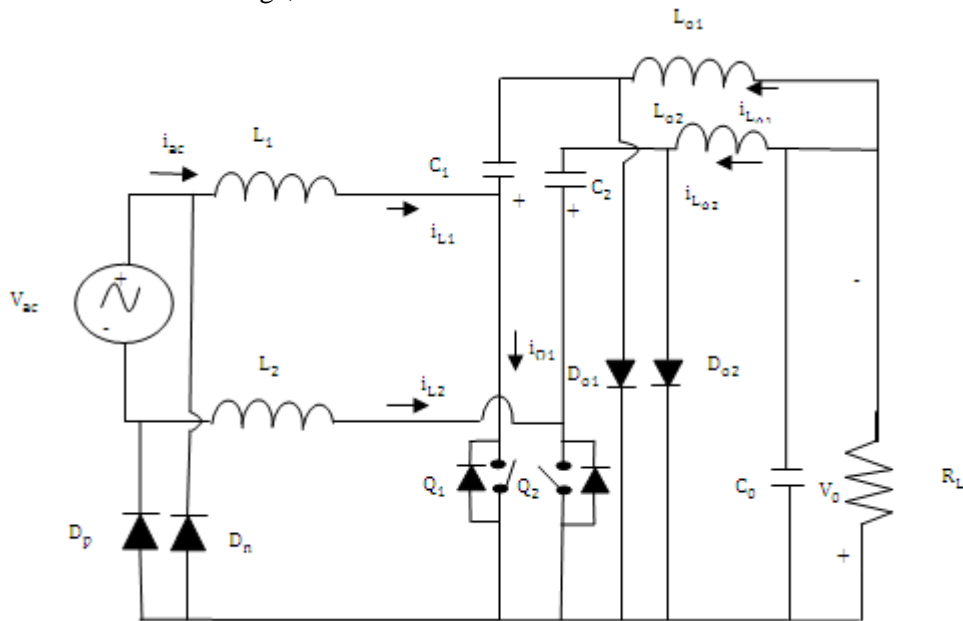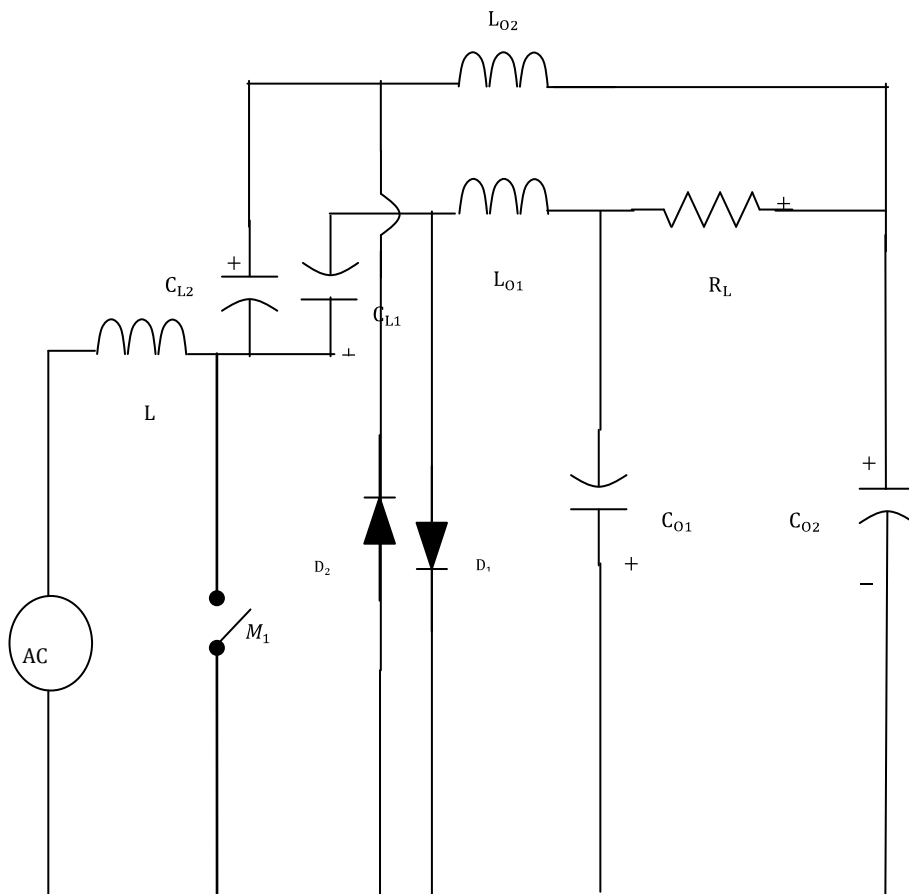

Fig.2. Conventional Cuk Converter

Fig.3. Proposed Cuk Converter Model

Table 1:Device Utility Comparison

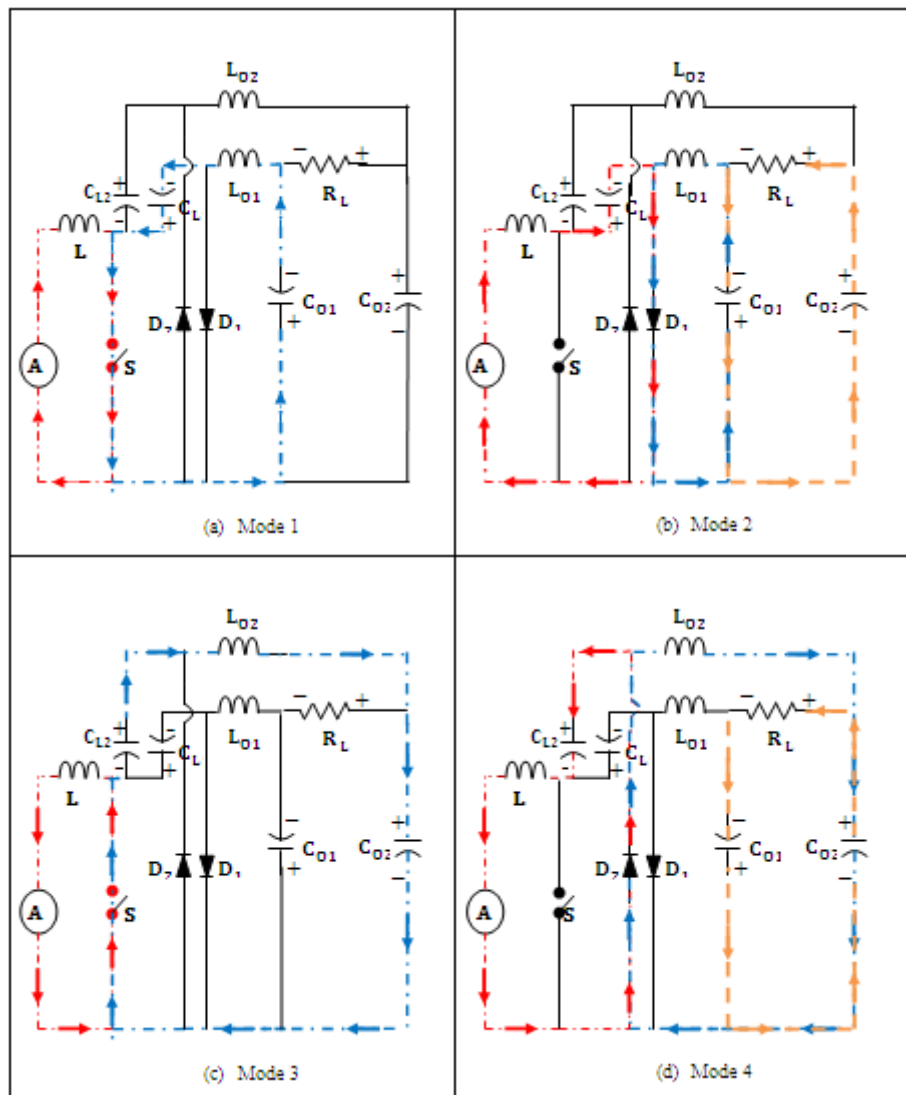| Bridgeless Converter Model	Switches	Diode	Capacitors	Inductors	Internal Diode across the switch/ Snubber Diode
Conventional Converter Model	2	4	3	4	2
Proposed Converter Model	1	2	4	3	None (Idle Switch)

Fig.4. Mode of Operation of the Proposed Bridgeless Cuk Converter

Mode 1: Here, the switch 'M_1' in the figure 4 is represented as 'S' for the operational mode description. This mode is initiated in the Positive Cycle of the AC supply and when the Switch 'S' is in ON condition. The inductance L is charged and the ground is attained through the drain and source of the Switch 'S' as shown in Fig. 5. Here, Switch 'S' represents the bidirectional switch with drain 'Dp' and Source 'Sp' during the positive cycle. Alternatively, the switch conducts with drain 'Dn' and Source 'Sn' during the negative cycle. During the circulating path, 'C_L1-S-C_01-L_01-C_L1' generated between the 1st ON and the next ON condition, the inductance 'L_01' is charged by the discharge of the inductance 'L' as shown in Fig. 4 (a).
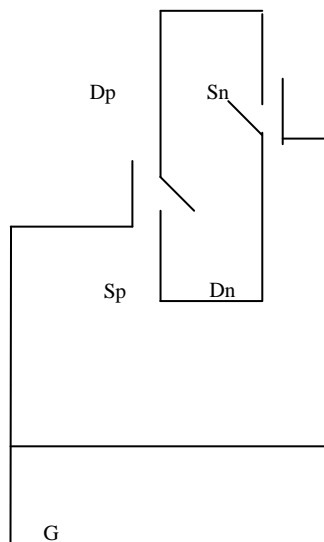

Fig.5. Bidirectional Switch 'S'

Mode 2: This mode occurs during positive cycle of the AC supply and when the Switch 'S' is in OFF condition. The main inductance L is charged and is stored in the capacitor as the voltage. Then, the current flows the diode D_1 and is grounded through the Vac neutral. Similarly, during the circulating path, '$L_{01} - D_1 - C_{01} - L_{01}$' the inductance '$L_{01}$' is charged. Then, the discharge of 'L_{01}' is completed through the load RL with the current flow, '$C_{01} - C_{02} - R_L - C_{01}$' as shown in Fig. 4 (b). During the connection with the Load, the capacitors C_{01} and C_{02} would be in series connection.

Mode 3: This mode is initiated in the negative cycle of the AC supply and when the Switch 'S' is in ON condition. The supply flows through the bidirectional switch 'Dn' and 'Sn'. Then, it charges the main inductance 'L' and gets grounded through the Vac neutral. During the circulating path, '$C_{L2} - L_{02} - C_{02} - S-C_{L2}$' the inductance '$L_{02}$' is charged by the discharge of the inductance 'L' as shown in Fig. 4 (c).

Mode 4: This mode occurs during negative cycle of the AC supply and when the Switch 'S' is in OFF condition. During this condition, the charge of inductance 'L' and the supply current Vac is added and flows through D_2 and stores the voltage in the capacitor C_{L2}. Similarly, during the circulating path, '$L_{02} - C_{02} - D_2 - L_{02}$' the inductance '$L_{02}$' is charged. Then, the discharge of 'L_{02}' is completed through the load RL with the current flow, '$C_{02} - R_L - C_{01} - C_{02}$' as shown in Fig. 4 (d). During the connection with the Load, the capacitors C_{01} and C_{02} would be in series connection.
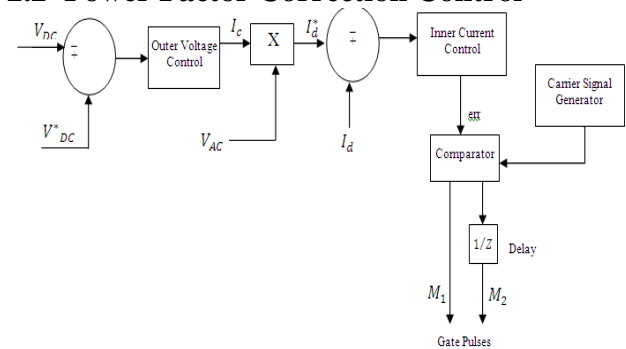
2.2 Power Factor Correction Control

Fig.6. Power Factor Correction Control diagram
The PFC control approach comprises of two controlling units namely the outer voltage control and the inner current control [18, 19]. The input to the outer voltage control is the PFC control scheme uses a current multiplier approach with a current control loop inside the speed control loop for continuous-conduction-mode operation of the converter. The control loop begins with the processing of voltage error obtained after the comparison of sensed dc link voltage (V_{DC}) and a voltage (V^*_{DC}) equivalent to the reference speed, through a proportional–integral (PI) controller to give the modulating control signal (I_c). This signal (I_c) is multiplied with a unit template of input ac voltage to get the reference dc current (I^*_d) and compared with the dc current (I_d) sensed after the power switches.

The resultant current error is amplified and compared with a saw tooth carrier wave of fixed frequency (f_s = 10 kHZ) generate the pulsewidth modulation (PWM) pulse for the Cuk converter [17, 20]. Its duty ratio (D) at a switching frequency (f_s) controls the dc link voltage at the desired value.

The dc link voltage of the PFC converter is given as

$$V_{DC} = V_{in} \frac{D}{(1 - D)}$$

2.3 PMSM Motor Modeling

The requisite of proper simulation of the system is the detailed model of PM motor drive system [21].

The development of the d-q model on rotor reference frame is well described by Fig. 7. At any time t, the rotating rotor d-axis makes an angle θ_r with the fixed stator phase axis whereas rotating stator mmf makes an angle α with the rotor d-axis. Both Stator mmf and the rotor rotates at the same speed.
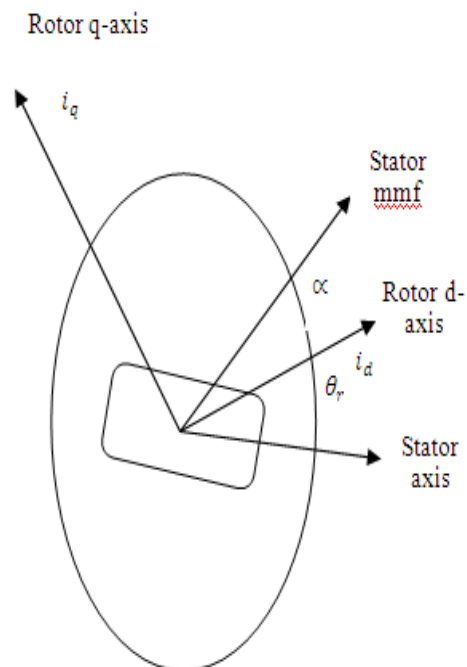

Fig.7. Motor Axis

The proper simultation of the system also necessitates the detailed modelling of PM motor drive system. The developed d-q model on rotor reference frame is shown in Fig. 7. At any time t, the rotating rotor d-axis makes and angle θr with the fixed stator phase axis and rotating stator mmf makes an angle α with the rotor d-axis. Here also, both Stator mmf and the rotor rotates at the same speed

The model of PMSM without damper winding has been developed on rotor reference frame using the following assumptions:

1) Saturation is neglected.

2) The induced EMF is sinusoidal.

3) Eddy currents and hysteresis losses are negligible.

4) There are no field current dynamics.

Voltage equations are given by:

$$V_q = R_s i_q + \omega_r \lambda_d + \rho \lambda_q \qquad (1)$$
$$V_d = R_s i_d - \omega_r \lambda_q + \rho \lambda_d \qquad (2)$$

Flux Linkages are given by

$$\lambda_q = L_q i_q \qquad (3)$$
$$\lambda_d = L_d i_d + \lambda_f \qquad (4)$$

Substituting equations 3 and 4 into 1 and 2

$$V_q = R_s i_q + \omega_r (L_d i_d + \lambda_f) + \rho L_q i_q \qquad (5)$$

$$V_d = R_s i_d - \omega_r (L_q i_q) + \rho (L_d i_d + \lambda_f) \qquad (6)$$

Arranging equations 5 and 6 in matrix form

$$\begin{pmatrix} V_q \\ V_d \end{pmatrix} = \begin{pmatrix} R_s + \rho L_q & \omega_r L_d \\ -\omega_r L_q & R_s + \rho L_d \end{pmatrix} \begin{pmatrix} i_q \\ i_d \end{pmatrix} \qquad (7)$$
$$+ \begin{pmatrix} \omega_r \lambda_f \\ \rho \lambda_f \end{pmatrix}$$

The developed torque motor is being given by

$$T_e = \frac{3}{2}\left(\frac{P}{2}\right)\left(\lambda_d i_q - \lambda_q i_d\right) \qquad (8)$$

The mechanical Torque equation is

$$T_e = T_L + B\omega_m + J\frac{d\omega_m}{dt} \qquad (9)$$

Solving for the rotor mechanical speed form equation 9

$$\omega_m = \int \left(\frac{T_e - T_L - B\omega_m}{J}\right) dt \qquad (10)$$

And

$$\omega_m = \omega_r \left(\frac{2}{p}\right) \qquad (11)$$

In the above equations ω_r is the rotor electrical speed where as ω_m is the rotor mechanical speed.

Table 2. Motor specification

Number of phases	3
Back Emf wave form	Sinusoidal
Rotor type	Salient-pole
Mechanical input	Torque Tm
Stator resistance (Rs)	2.8750
Inductances $(L_d(H) L_q(H))$	$8.5e^{-3}, 8.5e^{-3}$
Flux Linkage established by magnets	0.715
Inertia, friction factor, pole pairs	$1e^{-3}, 0, 4$

2.4 PMSM Vector Current Control Strategy

In this proposed approach, park transformation current control strategy is used to separate the active and reactive component from the overall current as shown in Fig. 8. Then, the reactive current is minimized to almost zero and the active current component is improved through the reference active current from capacitor voltage.

Park Transformation (abc to dqo)

Instantaneous active current component I_d is given by equation (12)

$$I_d = \frac{2}{3} * [I_a \; \sin(\theta) + I_b \sin\left(\theta - \frac{2\pi}{3}\right) \\ + I_c \sin\left(\theta + \frac{2\pi}{3}\right)] \tag{12}$$

Similarly, V_d can be obtained through the equation (12).

Instantaneous reactive current component I_q is given by equation (13)

$$I_q = \frac{2}{3} [I_a * \cos(\theta) + I_b * \cos\left(\theta - \frac{2\pi}{3}\right) \\ + I_c \cos\left(\theta + \frac{2\pi}{3}\right)] \tag{13}$$

Similarly, V_q can be obtained through the equation (13)

Zeroth Current

$$I_o = \frac{1}{3} [I_a + I_b + I_c \tag{14}$$

Similarly, V_0 can be obtained through the equation (14).

Where

I_a =Phase a inverter current, I_b = Phase b inverter current, I_c = Phase c inverter current, V_d =Instantaneous active voltage component, V_q =Instantaneous reactive voltage component, V_0 =Zeroth voltage component

2.5 Electrical Parameter Estimation

Park transformation performs rotating of rotor electrical position (reference frame) into DC values for transforming three-phase quantities into DC quantities.

The electrical rotor position is a mechanical rotor position divided by numbers of magnetic pole pairs 'pp'.

Generation of three phase AC voltages on motor terminals is been done after a control process so that by means of Park/Clarke transformations, DC values of the required/generated voltage must be transformed

$$I'_d = \left\{ \int \left[\frac{V_d}{L_d} - I_d * \frac{R_s}{L_d} + \omega_e * I_q \right] \right\} \tag{15}$$

$$I'_q = \left\{ \int \left[\frac{V_q}{L_q} - I_q * \frac{R_s}{L_q} - \omega_e * I_q \right. \right. \\ \left. \left. - \frac{\omega_e * F}{L} \right] \right\} \tag{16}$$

R_s denotes Stator resistance, L_d denotes d-axis self inductance, L_q q-axis self inductance, ω_e denotes estimated speed ; Frepresents Flux linkage =0.175.I_d denotes d-axis current, I_q denotes q-axis current.

2.6 Sensorless Speed and Theta estimation

Sensorless Control: The efficient performance of the PMS motor depends on the information on the rotor position however the shaft sensor for the rotor position tends to decrease the overall robustness and relaibiliyt of the system in some applications [22]. Hence, the goal of the system is to estimate the rotor position by some indirect techniques rather than using mechanical sensors for direct measurement of the rotor position. The approach of these kind of estimation techniques greatly vary depending on the position estimation or the motor type to which it is applied. For motors at low speed, special techniques like high frequency injection or not much efficient method called open-loop start-up are applied maximising the speed of spinning the motor such that BEMF observer gets appreciably higher BEMF. The proper operation in sensorless mode requires atleast 5 percent of the base speed. However for high speed, a BEMF observer in d/q reference frame is used. To get a essential number of phase current samples and DC bus voltage, the PWM frequency and control loop should be high

$$\omega_e = I_d * I'_q - I_q * I'_d - \left[\frac{\left(I_q - I'_q\right) * F}{L} \right] * \\ \left[\left(K_p + \int K_i \, dt \right) \right] \tag{17}$$

$$\theta = \int \omega_e . \, dt \tag{18}$$

Moreover, the sensorless estimation of speed and theta entirely depends on the motor parameters such as stator resistance, flux linkage and self inductance (d and q axis).

2.7 Reference current estimation

Here, the error difference between the estimated speed and the reference speed of the motor is obtained from the following equation.

$$i^*q = \left(K_p + \int K_i \, dt \right) E\omega_r \tag{19}$$

i^*q reference q-axis current through which the reactive current may be controlled using proportional integral gain effectively. In the mean time, reference d-axis reference current (i*d) becomes zero.

2.8 Electrical Parameter Estimation

In vector control process, the error between actual and reference q-axis current is the reference q axis voltage.

$$V^*q = \left(K_p + \int K_i \, dt \right) EI_q \tag{20}$$

$$V^*d = \left(K_p + \int K_i \, dt \right) EI_d \tag{21}$$

Similarly, the error between actual and reference d-axis current is the reference d axis voltage.
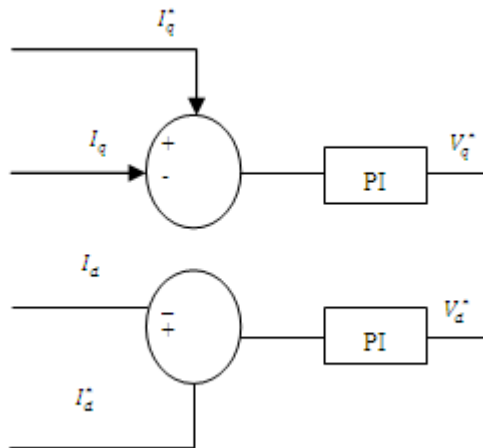
Fig.8. Error between actual and reference d-axis current is the reference d axis voltage

The magnitude of the reference voltages are entirely based on the saturation limit (upper/lower), Proportional gain and Integral gain of the PI controller.

2.9 Reference voltage estimation

After estimating the reference voltages V_α and V_β coordinates, inverse park transformation is applied.

Inverse Park Transformation (dq0 to abc)

Reference Voltage V_a

$$V_a = V_d * sin(\theta) + V_q * cos(\theta) + V_0 \qquad (22)$$

Reference Voltage V_b

$$V_b = V_d * sin\left(\theta - \frac{2\pi}{3}\right)$$
$$+ V_q * cos\left(\theta - \frac{2\pi}{3}\right) + V_0 \qquad (23)$$

Reference Voltage V_c

$$V_c = V_d * sin\left(\theta + \frac{2\pi}{3}\right)$$
$$+ V_q * cos\left(\theta + \frac{2\pi}{3}\right) + V_0 \qquad (24)$$

After applying inverse park transformation, two phase d-q coordinates is transformed into three phase voltage references V_{abc}. The attained reference voltage V_{abc} is compared with the carrier signal and its gate pulses are given to the VSI.

2.10 PWM Control Strategy

The widely used PWM current controllers are based on the principle of comparison of a triangular carrier wave of desire switching frequency in which the switching frequency if kept constant and compared with the error of the controlled signal. The generation of the sum of the reference signal in the controller and the negative actual motor current together constitute the error of the controlled signal. The comparison provides the voltage control signal which gets transferred to the gates of the voltage source inverter for generating the desired output. The response of the control will be based on the

error. The switch of the inverter leg goes to the positive polarity (upper switch ON) if the error command is greater than the triangle waveform whereas it goes to the negative polarity (lower switch on) for error command lesser than the triangle waveform. This operation helps for generating PWM signal as shown in Fig. 9. An output voltage is produced in proportionality to the current error command when the inverter leg is forced to switch at the frequency of the triangle wave. This work is based on the procedure of Space Vector Pulse Width Modulation (SVPWM) as the current control technique. The inputs to SVPWM are the voltage references V_a, V_b and V_c

In space vector PWM, three switches are independent among its six switches and those are integrated to provide eight feasible space voltage vectors [23].
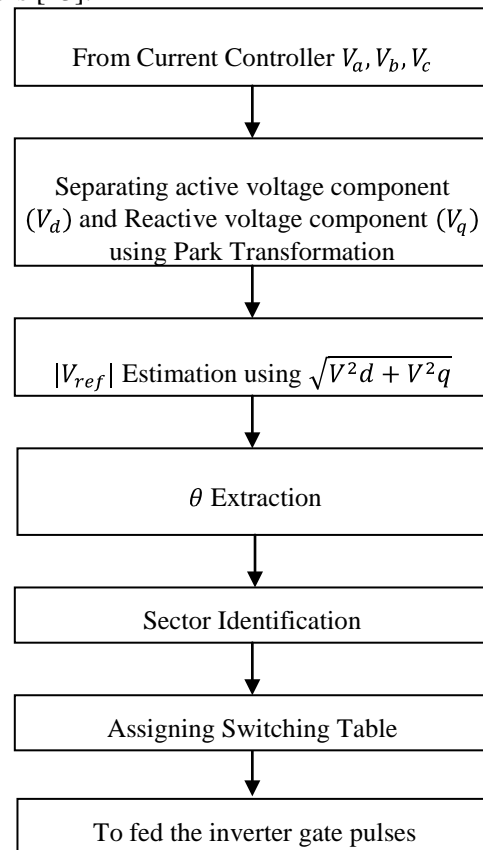

Fig.9. Working of SVPWM

The inverter output voltage is been controlled by PWM for considerable minimisation of THD. PWM is also used for elimination of lower order harmonics as many of the filters like LC, LCL do not perform this elimination. Inspite of these advantages of PWM, its inherent drawbacks are as follows:

- The elimination of 3rd and 5th order harmonics is not much effective

- The higher PWM frequency leads to increase of the power losses along the switches
- Electromagnetic Interference (EMI) problem will be arised due to higher order harmonics in the current.

These limitations of the PWM approaches have made the improved PWM techniques as an attractive research solution. This work employs SVPWM and its working is shown in Fig. 7.The input from the current controller [24, 25] is taken as the reference sine from SVPWM. Park transformation is used to separate the instantaneous active voltage component (Vd) and instantaneous reactive voltage component (Vq) from the grid voltage.

The estimation of magnitude of V_d and V_q is given by $|V_{ref}|$. Then, angle θ is extracted from the active and reactive voltage component and the attained angle is compared with the angles such as $\left(-\frac{2\pi}{3}, -\frac{\pi}{3}, 0, +\frac{\pi}{3}, +\frac{2\pi}{3}\right)$ for identifying the appropriate sector for that angle. Thus, each sector represents 60^0 as shown in Fig. 7.
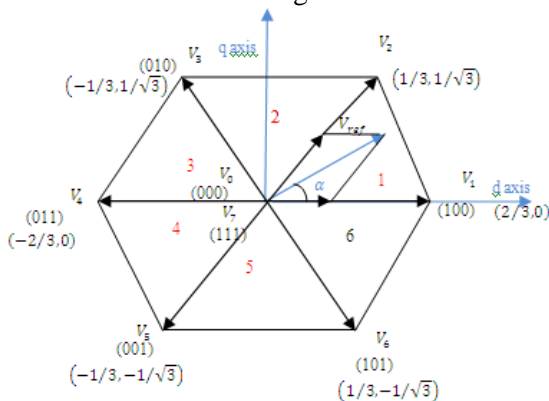

Fig.10. Basic switching vectors and sectors

The basic switching vectors and sectors in SVPWM [26] is shown in Fig. 10. The average of the adjacent vectors in each vector of SVPWM is taken. Then, the two adjacent vectors and zero vectors are combined to generate the appropriate PWM signals. Finally, the corresponding switching time vector is assigned based on the identified sector and shown below:

Table 3. Switching Time Vector

Sector	Upper Switches (S_1, S_3, S_5)	Lower Switches (S_2, S_4, S_6)
1	$S_1 = T_1 + T_2 + (0.5 \times T_0)$ $S_3 = T_2 + (0.5 \times T_0)$ $S_5 = (0.5 \times T_0)$	$S_4 = (0.5 \times T_0)$ $S_6 = T_1 + (0.5 \times T_0)$ $S_2 = T_1 + T_2 + (0.5 \times T_0)$
2	$S_1 = T_1 + (0.5 \times T_0)$ $S_3 = T_1 + T_2 + (0.5 \times T_0)$ $S_5 = (0.5 \times T_0)$	$S_4 = T_2 + (0.5 \times T_0)$ $S_6 = (0.5 \times T_0)$ $S_2 = T_1 + T_2 + (0.5 \times T_0)$
3	$S_1 = (0.5 \times T_0)$ $S_3 = T_1 + T_2 + (0.5 \times T_0)$ $S_5 = T_2 + (0.5 \times T_0)$	$S_4 = T_1 + T_2 + (0.5 \times T_0)$ $S_6 = (0.5 \times T_0)$ $S_2 = T_1 + (0.5 \times T_0)$
4	$S_1 = (0.5 \times T_0)$ $S_3 = T_1 + (0.5 \times T_0)$ $S_5 = T_1 + T_2 + (0.5 \times T_0)$	$S_4 = T_1 + T_2 + (0.5 \times T_0)$ $S_6 = T_2 + (0.5 \times T_0)$ $S_2 = 0.5 \times T_0$
5	$S_1 = T_2 + (0.5 \times T_0)$ $S_3 = (0.5 \times T_0)$ $S_5 = T_1 + T_2 + (0.5 \times T_0)$	$S_4 = T_1 + (0.5 \times T_0)$ $S_6 = T_1 + T_2 + (0.5 \times T_0)$ $S_2 = (0.5 \times T_0)$
6	$S_1 = T_1 + T_2 + (0.5 \times T_0)$ $S_3 = (0.5 \times T_0)$ $S_5 = T_1 + (0.5 \times T_0)$	$S_4 = 0.5 \times T_0$ $S_6 = T_1 + T_2 + (0.5 \times T_0)$ $S_2 = T_2 + (0.5 \times T_0)$

2.11 Time duration determination

The time duration, T_1, T_2 and T_z are clearly depicted in Fig. 13. The formulations to determine the time durations are also evaluated [27].

$$T_1 = k \times \left(\sin\left(\frac{\pi}{3} - \theta + \frac{n-1}{3}\pi\right)\right)$$

$$T_2 = k \times \left(\sin\left(\theta - \frac{n-1}{3}\pi\right)\right) \quad (25)$$

$$T_0 = T_z - (T_1 + T_2)$$

Where, Modulation index 'k' is defined as

$$k = \frac{\sqrt{3} \times T_z \times V_{ref}}{V_{dc}} \quad (26)$$

$T_z = \frac{1}{f_s}$; f_s = switching frequency (10 kHz)

2.12 Three Phase Inverter

The gate pulses attained from the SVPWM is fed as input to the three phase inverter. Voltage Source Inverters are devices that convert a DC voltage to AC voltage of variable frequency and magnitude. They are very commonly used in adjustable speed drives and are characterized by a well defined switched voltage wave form in the terminals [27]. Fig. 8 shows a voltage source inverter.

Three phase inverters consisting of six power switches are connected to a DC voltage source as shown in Fig. 11. Based on the requirements of operation, ratings and the application, the inverter switches must be carefully selected. Nowadays several devices such as thyristors, bipolar junction transistors (BJTs), MOS field effect transistors (MOSFETs), insulated gate bipolar transistors (IGBTs) and gate turn off thyristors (GTOs) are also available. Industries mostly prefer MOSFETs because of its high power gain and control offered by Metal Oxide Semiconductor (MOS) gating permits. MOSFET is also considered as a universal power device for low power and low voltage applications and hence the application of it is best suited in this work.

The rotation of the motor is possible by sending the output of the VSI to the PMSM. The control of the motor speed using PI controller is the main focus of this work. The performance of the motor based on varying the load torque is also been analysed for deriving the relation between the torque and speed.
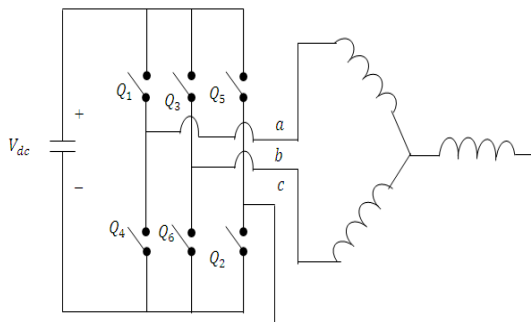

Fig.11. Three phase inverter

3 Simulation Results

The proposed system has been simulated using MATLAB 2011a for the following input and output data specifications: V_{ac} = 100 Vrms , Vo = 48V, and fs = 50 kHz.
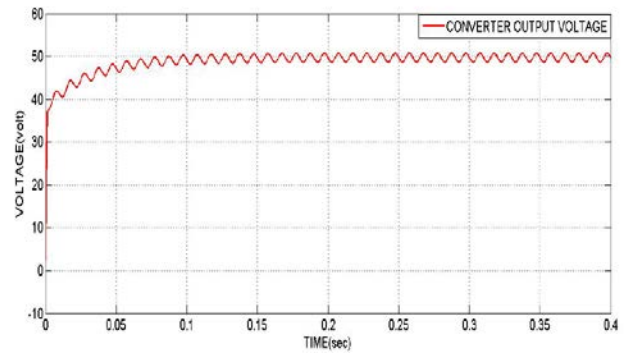
3.1 Converter Results

Fig.12. Converter Voltage

Fig. 12 shows the proposed cuk converter output voltage. It is clearly observed from the Fig. that a constant 48 V is attained by the proposed converter model. Even though there are slight variations in the initial time period, at 0.15 seconds, the proposed converter voltage gets constant at 48 V at 4 Nm torque and 1500 rpm.
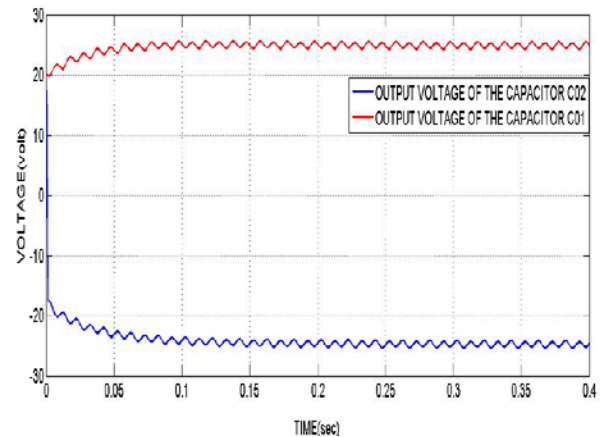

Fig.13. Converter Capacitor Voltage

Fig. 13 shows the output capacitor voltage of the converter. Capacitors C_{01} and C_{02} produces 24 V respectively. When connected with the load, both the capacitors form a series connection which in turn results in 48 V (24V+24V) as shown in the mode of operation.
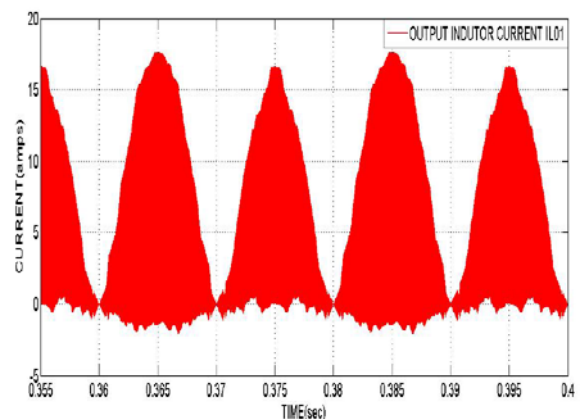

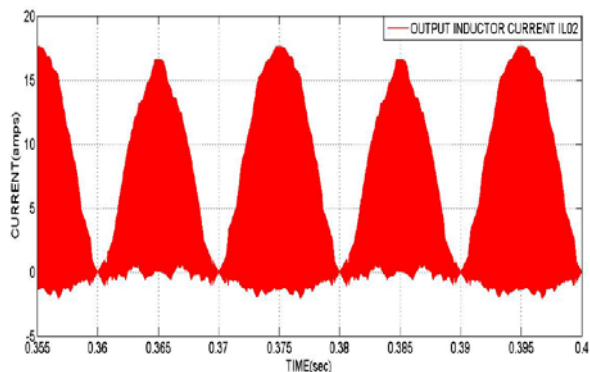Fig.14. Converter Inductor Current L_{01}

Fig.15. Converter Inductor Current L_{O2}

Fig. 14 and 15 show the output inductor ripple current IL_{O1} and IL_{O2} respectively. During the positive cycle, a circulating path is created in which if L_{O1} is in charging condition, then L_{O2} will be in discharging condition. Alternatively, during the negative cycle, L_{O2} is in charging condition and L_{O1} will be in discharging condition.
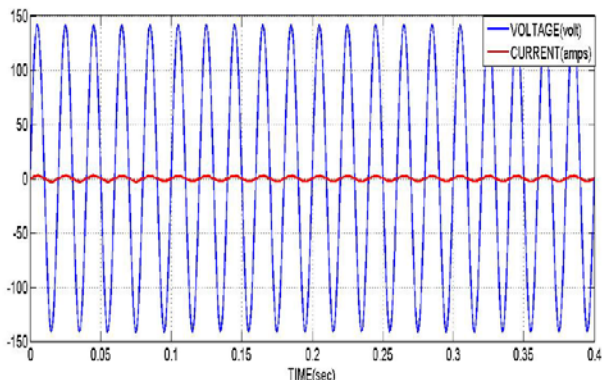

Fig.16. Voltage-Current In phase Waveform

Fig. 16 shows the voltage-current in phase waveform of the proposed converter model. It is observed from the Fig. that the angle between voltage and current is zero. The current obtained is approximately 5 Amps. The proposed converter model attains almost unity power factor through the following equation.

$$\text{Power Factor (PF)} = \left| \frac{P}{\sqrt{P^2 + Q^2}} \right|$$

Where, P and Q represents active and reactive power respectively.

3.2 PMSM Motor Results

The proposed research work focuses on enhancing the stability parameters of Speed and Torque (Rise time, Peak time Maximum overshoot, Settling time. The performance of different control techniques have been compared based on the obtained results.
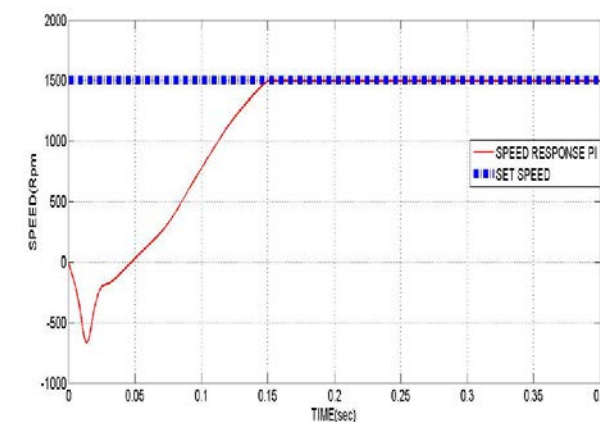
## 3.3 No Load Condition
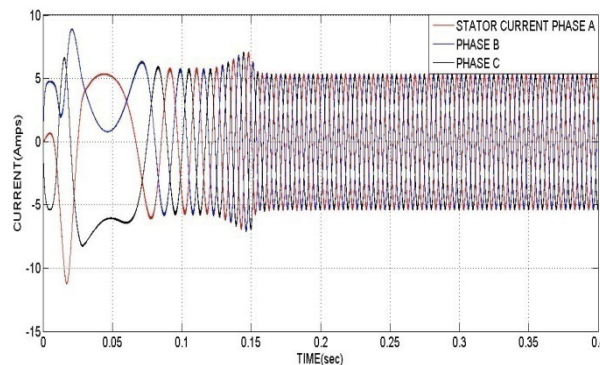
Current (Amps)
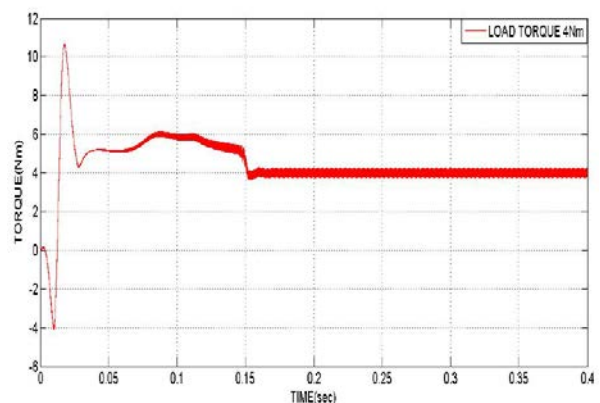
Torque Nm

Speed (rpm)

Fig.17. No Load Condition of PMSM (Current, Torque and Speed)

Fig. 17 (a), (b) and (c) shows the current, torque and speed of the PMSM respectively in no load condition. With the constant torque and speed of 4 Nm and 1500 rpm respectively, the stator current of the PMSM attained is 5 Amps as shown in Fig. 17 (a). During the initial time periods (between 0 and 0.1 seconds), there is slight fluctuation in the PMSM response. This is mainly due to the sensorless feedback of the PMSM. However, the current gets constant at 0.15 seconds with 5 Amps.

Similarly, the response of torque and speed are clearly shown in Fig. 17 (b) and (c) respectively. Fig. 17 (c) shows the speed response of the proposed approach with negligible peak overshoot.

Thus, the proposed approach is observed to produce significant response in terms of current, torque and speed.
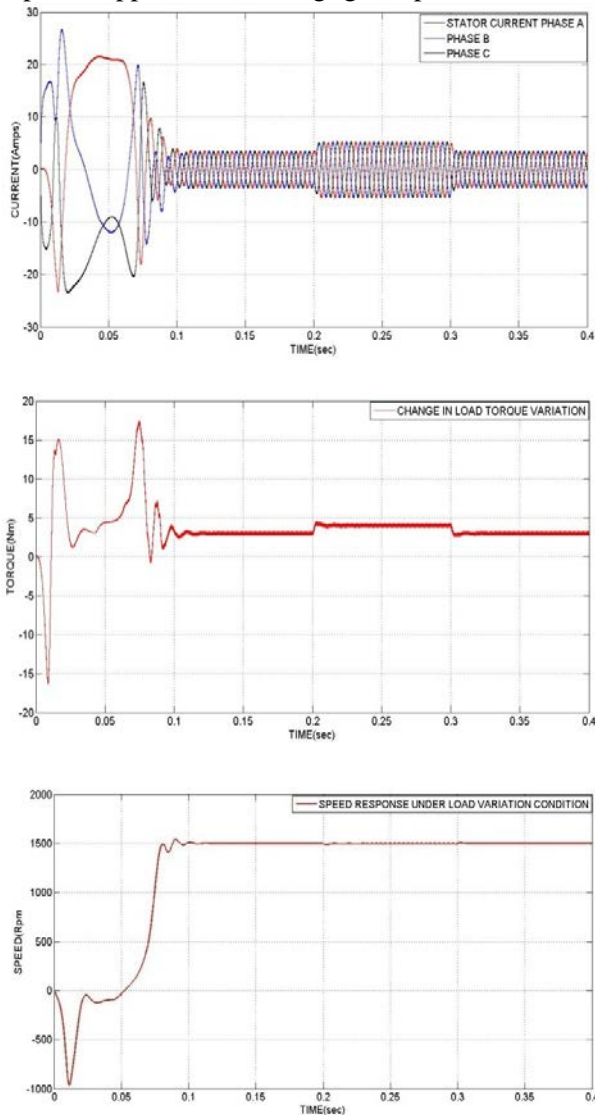
(a)Load Torque Variation
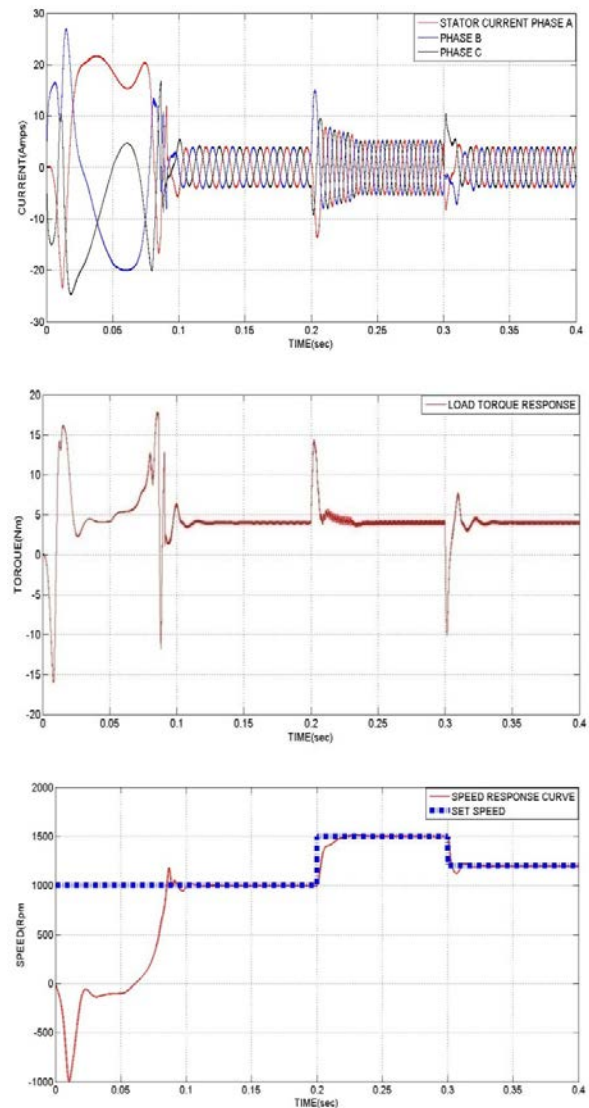
(b)Sudden change in Speed

Fig.18. Performance Analysis of Proposed System

(Current, Torque and Speed Response of PI Controller)

Fig. 18 shows the performance analysis of the proposed system model. The Fig. 18 (a) shows the load torque variation of the proposed system. With the sudden change in load, the current varies but the speed is kept constant at 1500 rpm. Initially, the PMSM is operated at 3 Nm torque upto 0.2 seconds. At this point, the stator current obtained is 3 Amps. Then, between 0.2 and 0.3 seconds, the load torque is suddenly varied to 4 Nm torque and the stator current response obtained is 5 Amps. Similarly, when the load torque is varied to 3 Nm between 0.3 and 0.4 seconds, the stator current response is

observed to be 3 Amps. But, in all the above cases, the speed is maintained constant at 1500 rpm with negligible peak overshoot even at the load torque variation between 0.2 and 0.4 seconds.

Fig. 18 (b) shows the current and torque response of the proposed system for varying speed condition. The speed of the PMSM is maintained at 1000 rpm till 0.2 seconds. Then, between 0.2 and 0.3 seconds, the speed is varied and maintained at 1500 rpm. Similarly, between 0.3 and 0.4 seconds, the speed of PMSM is again varied to 1200 rpm. At these

varying conditions, the torque and stator current response of the PMSM is evaluated.
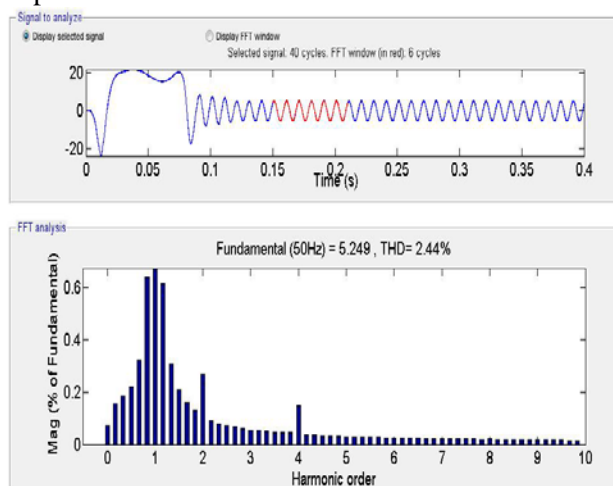

Fig.19. THD at 1500 rpm, 155 V_{rms}

Table 4: Performance Evaluation under Speed Variation Condition at 155 V_{rms}

Speed (Rpm)	THD (%)	PF	Stator Current (Amps)
1000	2.82	0.9991	3.9
1500	2.44	0.9995	5.2
1200	2.68	0.9992	4.1

Table 4 shows the performance evaluation of the THD and PF response under speed variation condition at 155 V_{rms}. It is clearly observed from the table that when the speed is decreased from the normal condition, current decreases and voltage increases which in turn decreases the pulse width of the inverter gate pulses. So, the filter design may not be able to sufficiently support the current ripples which in turn increase the THD. The load current variation would result in supply current change which results in minimum angle shifting of the voltage and current. Thus, the PF values also decreases.

Table 5: Performance Evaluation under Input Voltage Variation Condition at 1500 Rpm

Supply Voltage (V_{rms})	THD (%)	PF	Stator Current (Amps)
145	2.25	0.9997	6
155	2.44	0.9995	5.2
165	2.62	0.9993	4.4

Table 5 shows the performance evaluation of the THD and PF response under input voltage variation

condition at 1500 Rpm It is clearly observed from the table that when the supply voltage is varied, current increases which in turn increase the pulse width of the inverter gate pulses. So, the filter design may not be able to sufficiently support the current ripples which in turn increase the THD. When the supply voltage is decreased from the nominal voltage, the THD gets decreased and PF gets increased. But, when supply voltage is increased, THD is increased and PF is decreased.

4 Conclusion

This work proposes a novel design of cuk converter model with buck mode operation for high power application. The design of novel cuk converter with lesser number of power devices, active and passive components is the main contribution of this work. This model makes employs only ten utility devices rather than 15 electronic utility devices as that of the conventional bridgeless cuk converter thus eliminating the major switching losses. The SVPWM control technique used in this work is effective as it eliminates the lower order harmonics which is clearly reflected in the THD of the proposed work. The THD attained by the proposed work is 2.44% at 1500 Rpm. Also, the proposed converter model tends to attain power factor of almost unity. The simulation results are carried out with varying speed and load conditions of the PMSM. The constant speed of 1500 rpm even with the sudden change in load is been maintained by this proposed system. The load torque is also maintained constantly even with sudden speed change and with lesser peak overshoot.

References:
[1] Kai Wan, Jingsheng Liao, M. Ferdowsi, " Control Methods in DC-DC Power Conversion - A Comparative Study", In proceeding of: Power Electronics Specialists Conference, 2007. PESC 2007.
[2] Vashist Bist and Bhim Singh, "An Adjustable-Speed PFC Bridgeless Buck–Boost Converter-Fed BLDC Motor Drive", IEEE TRANSACTIONS ON INDUSTRIAL ELECTRONICS, VOL. 61, NO. 6, JUNE 2014.
[3] Aysha Kemaidesh AL-Kaabi, Abbas A. Fardoun and Esam H. Ismail, "High efficiency Bridgeless Unity Power factor CUK converter Topology", International Conference on Renewable Energies and Power Quality, 2013.

[4] R.-L. Lin and H.-M. Shih, "Piezoelectric transformer based current-source charge-pump power-factor-correction electronic ballast," IEEE Trans.Power Electron., vol. 23, no. 3, pp. 1391–1400, May 2008.

[5] L. Huber, Y. Jang, and M. Jovanovic, "Performance evaluation of bridgeless PFC boost rectifiers," IEEE Trans. Power Electron., vol. 23, no. 3,pp. 1381–1390, May 2008.

[6] Govindaraj Thangavel, Debashis Chatterjee, and Ashoke K. Ganguli, "Design, Development and Control of an Axial Flux Permanent Magnet Linear Oscillating Motor using FE Magnetic Analysis Simulation Models," Int. Journal of Electrical and Electronics Engineering, Oradea, Romania, October 2010

[7] R.Narmatha and T.Govindaraj, "Inverter Dead-Time Elimination for Reducing Harmonic Distortion and Improving Power Quality", International journal of Asian Scientific Research, vol.3, April 2013.

[8] Srikant Misra, Sujit Kumar Patro, Debasis Mahapatra, Partha Sarathi Mansingh, "Implementation Of DC-DC Buck Converter With Switched Mode Control Technique For Enhancement of Efficiency of Solar Cell", International Journal of Scientific & Engineering Research, Volume 4, Issue 7, July-2013, 1450.

[9] A.S. Oshaba, and E. S. Ali, "Bacteria Foraging: A New Technique for Speed Control of DC Series Motor Supplied by Photovoltaic System", International Journal of WSEAS Transactions on Power Systems, Vol. 9, 2014, pp. 185-195.

[10] A.S. Oshaba, and E. S. Ali, "Speed Control of Induction Motor Fed from Wind Turbine via Particle Swarm Optimization Based PI Controller", Journal of Applied Sciences, Engineering and Technology (Maxwell Science Publication), Vol. 5, No. 18, May 2013, pp. 4594-4606.

[11] A. S. Oshaba, and E. S. Ali, "Swarming Speed Control for DC Permanent Magnet Motor Drive via Pulse Width Modulation Technique and DC/DC Converter", Research Journal of Applied Sciences, Engineering and Technology (Maxwell Science Publication), Vol. 5, No. 18, May 2013, pp. 4576-4583.

[12] Aysha Kemaidesh AL-Kaabi, Abbas A. Fardoun and Esam H. Ismail, High efficiency Bridgeless Unity Power factor CUK converter Topology', International Conference on Renewable Energies and Power Quality (ICREPQ'13), No.11, March 2013

[13] D.Sarith , B.M.Manjunatha , 'PFC Applications based on new Ac--Dc Bridgeless Cuk Rectifiers' IJREAT International Journal of Research in Engineering & Advanced Technology, Volume 1, Issue 6, Dec-Jan, 2014

[14] M. Brkovic and S. Cuk, "Input current shaper using Cuk converter," in Proc. Int. Telecommun. Energy Conf., 1992, pp. 532–539.

[15] D. S. L. Simonetti, J. Sebastian, and J. Uceda, "Design Criteria for Sepic and Cuk Converters as Power Factor Preregulators in Discontinuous Conduction Mode," IEEE Trans. Ind. Electron., vol. 44, no. 5, pp. 283–288, 2009.

[16] Nesapriya. P., S. Rajalaxmi, 'Closed Loop Control of Bridgeless Cuk Converter Using Fuzzy Logic Controller for PFC Applications', World Academy of Science, Engineering and Technology International Journal of Electrical, Robotics, Electronics and Communications Engineering, vol.7, no.11, pp.1042-1047, 2013

[17] Shalini.K, Murthy.B, 'An Efficient Closed Loop Controlled Bridgeless Cuk Rectifier For Pfc Applications', International Journal Of Innovative Research In Electrical, Electronics, Instrumentation And Control Engineering, Vol. 2, Issue 2, February 2014

[18] Abbas A. Fardoun, Esam H. Ismail, Ahmad J. Sabzali, and Mustafa A. Al-Saffar, "New Efficient Bridgeless Cuk Rectifiers for PFC Applications", IEEE Transactions On Power Electronics, vol. 27, no. 7, July 2012

[19] Y. Jang and M. Jovanovic, "A bridgeless PFC boost rectifier with optimized magnetic utilization," IEEE Trans. Power Electron., vol. 24, no. 1, pp. 85–93, Jan. 2009.

[20] Sanjeev Singh and Bhim Singh, "A Voltage-Controlled PFC Cuk Converter-Based PMBLDCM Drive for Air-Conditioners", IEEE TRANSACTIONS ON INDUSTRY APPLICATIONS, VOL. 48, NO. 2, MARCH/APRIL 2012.

[21] C.Balaji, C.H. Jayavardhan Rao, M. Karthik, "An Integrated Step-Down Converter using Sngle-Stage Single-Switch", Research Inventy: International Journal Of Engineering And Science, Vol.3, Issue 1 (May 2013), PP 37-50.

[22] Sheng-Yu T, Hung-Yuan W. "A Photovoltaic Power System Using a High Step-up Converter for DC Load Applications", 2013.

[23] Van der Broeck HW. "Analysis of the harmonics in voltage fed inverter drives caused by PWM schemes with discontinuous switching operation". EPE, Firenze, Italy, 1991; 261–266.

[24] Enrique L. Carrillo Arroyo, "Modeling and Simulation Of Permanent Magnet Synchronous Motor Drive System", 2006.

[25] José Carlos Gamazo-Real,* Ernesto Vázquez-Sánchez, and Jaime Gómez-Gil, "Position and Speed Control of Brushless DC Motors Using Sensorless Techniques and Application Trends", Sensors (Basel). 2010; vol.10, no.7, pp.6901–6947.

[26] Nasrudin A. Rahim, Jeyraj S. Multistring "Five-Level Inverter with Novel PWM Control Scheme for PV Application", IEEE Trans. Ind. Electron, 2010; 57: 2111–2123.

[27] B. K. Bose, "Power Electronics and Variable Frequency Drives":, 1 ed: Wiley, John & Sons, 1996.